ACS OMEGA

http://pubs.acs.org/journal/acsodf

Article

Study on the Effect of Threshold Pressure Gradient on Remaining Oil Distribution in Heavy Oil Reservoirs

Wenli Ke, Yuetian Liu,* Xu Zhao, Gaoming Yu,* and Jie Wang

Cite This: *ACS Omega* 2022, 7, 3949−3962

Read Online

ACCESS | Metrics & More | Article Recommendations

ABSTRACT: Due to the spatial network structure, heavy oil has a high threshold pressure gradient when it flows through porous media, and the threshold pressure gradient plays a crucial role in the distribution of remaining oil. In previous study, the common methods to measure the threshold pressure gradient include the microflow-established differential pressure (MFEDP) method, capillary equilibrium method, and the percolation curve fitting method. In this study, a sample from the SZ36-1 oilfield was analyzed for the basic physical properties based on the comparison of the previous measurement to study the influence of mobility on the threshold pressure gradient and then an independently developed numerical simulator was established to study the effect of the threshold pressure gradient on the remaining oil distribution considering the permeability range, crude oil viscosity, well network deployment, well spacing, and fluid recovery rate. The results show that the SZ36-1 oilfield fluid belongs to Bingham fluids with yield stress and the mobility having an exponent relation to the threshold pressure gradient based on the measurement of the MFEDP method. Considering the threshold pressure gradient of heavy oil, the uneven distribution of remaining oil is intensified and the remaining oil is enriched. This study provides a reference for efficient development of heavy oil reservoirs.

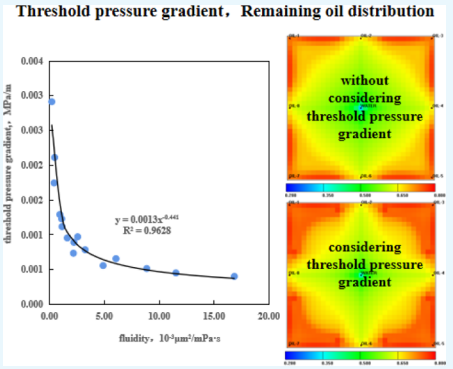

1. INTRODUCTION

Heavy oil reservoirs are widely distributed in the world, and as an important part of the world's oil resources heavy oil plays a pivotal role in exploration and development. The outstanding feature of heavy oil is that the content of colloids and asphaltene is high and the light fraction is small. Moreover, with the increase of the content of colloids and asphaltene, the relative density and viscosity of heavy oil also increase, and the heavy oil shows the characteristics of Bingham fluids.[1] The interaction between asphaltene molecules endows the heavy oil with structural and mechanical properties and non-Newtonian fluid characteristics.[2] At present, it has been found that in the process of the water drive recovery stage, only when the pressure gradient is greater than the threshold pressure gradient, viscous oil can start to flow due to its structural and mechanical properties of heavy oil.[3] Thomas et al. proposed that the minimum displacement pressure in porous media is the ultimate pressure (threshold pressure).[4] Moreover, this had been further proved by Boronin et al., with field data and lab experiments.[5] Therefore, it is of great theoretical significance to study the properties of heavy oil, the measurement method of the threshold pressure gradient, and the influence of the threshold pressure gradient on the distribution of remaining oil.

Ma et al. studied the rheology of heavy oil in detail and pointed out that it performed as a Newtonian fluid above the critical temperature and a Bingham fluid under the critical temperature. The critical temperature is the temperature transition point of heavy oil from Newtonian fluid properties to Bingham fluid properties and is the lowest temperature point at which heavy oil exhibits Newtonian fluid properties.[6−9] In 1972, Wang found through the study on rheological properties of heavy oil that heavy oil has a certain yield stress, that is, when the shear stress is less than the yield stress, heavy oil in the large space network structure has no obvious damage, whereas when the shear stress exceeds the yield stress, the network structure was damaged, losing the structure and mechanical properties of heavy oil and becoming a Newtonian fluid.[10,11] Therefore, in the process of water flooding of heavy oil, within the scope of the smaller pressure gradient, the structure of the heavy oil is not destroyed and only creeping or no flow occurs, whereas when the pressure gradient is increased to the extent of causing destruction of the heavy oil structure, the heavy oil begins to flow, and the fluid flow velocity and the pressure gradient present a quasi-linear relationship. It is generally considered that the pressure gradient corresponding to the failure of the heavy oil structure is the threshold pressure gradient.[12,13] Chen et al.

Received: August 19, 2021
Accepted: December 24, 2021
Published: January 26, 2022

proposed that due to the three-dimensional structure, the Bingham fluid has yield stress and needs the threshold pressure gradient to flow in porous media.[14−16]

At present, there are many experimental methods to determine the threshold pressure gradient worldwide, but there is no unified standard. Tian et al. used the percolation curve fitting (PCF) method to obtain the threshold pressure gradient.[17] The capillary equilibrium (CE) method adopted by Song et al. applied the theory of communicating vessels. When measuring the threshold pressure gradient, a capillary is connected at the inlet and outlet ends of the core, and the fluid flows from the inlet end to the outlet end under the gravity until it reaches a height difference, which is the minimum threshold pressure of the sample.[18,19] Tan et al. used the unsteady method by establishing the unstable percolation equation and solving it numerically with the finite difference method, then the threshold pressure gradient was obtained by regression.[20] The CE method established by Li Ai-fen is to flood at a small flow rate until the fluid in the core begins to flow, then turn off the liquid intake switch, and record the balanced pressure as the threshold pressure.[21] The measurement results of heavy oil threshold pressure gradient are different. Therefore, it is necessary to study the current methods of heavy oil threshold pressure gradient and screen out a more accurate and efficient measurement method.

In addition, the percolation law of heavy oil reservoirs does not conform to Darcy's law in the actual development of the oilfield, which affects the distribution of remaining oil. Therefore, on the basis of revising the previous percolation model, the influence of the threshold pressure gradient on the distribution of remaining oil in heavy oil was studied numerically. Xi proposed that the non-Darcy flow of heavy oil is mainly caused by abnormal oil viscosity, which is manifested in two aspects: (1) the higher the viscosity of the heavy oil, the thicker the boundary layer, the more obvious the plastic flow, and the greater the viscous force between heavy oil and pores, consistent with the properties of Buckingham fluids; (2) the threshold pressure gradient is controlled by the interaction between the solid and liquid interface. The higher the oil viscosity, the stronger the polarity, the greater the viscous force, and the larger the contact area with the pores.[22,23] Cheng and Prada et al. established a mathematical model of an oil−water two-phase non-Darcy flow based on the pseudo-threshold pressure gradient motion equation.[24,25] Dmitriev studied the correlation between the minimum threshold pressure gradient at the macrolevel and the heterogeneity parameters at the microlevel by considering the progressive properties of the macroscopic flow law at large and small rates and designed the Bingham plastic non-Darcy flow considering inertia loss.[26] Han and Balhoff et al. established a three-dimensional and three-phase mathematical model considering the pseudo-threshold pressure gradient based on indoor physical simulation experiments and basic theoretical research.[27−29] By assuming that the oil−water pseudo-threshold pressure gradient is a function of the permeability of the medium and the water diversion coefficient, Zhao et al. established the non-Darcy equation. Then, the numerical simulation of the variable threshold pressure gradient based on the black oil simulator was realized,[30] which to some extent compensates for the deficiency of the Darcy flow numerical simulation method. However, the threshold pressure gradient in the mathematical model should be considered as a variable because it changes with mobility, and the actual reservoir is heterogeneous.

The threshold pressure gradient of heavy oil directly affects the remaining heavy oil. The remaining heavy oil consists of the crude oil in the dead oil zone that is not affected and the remaining oil that is affected but still cannot be driven out.[31] Near the well, the pressure gradient is the highest. With the increase of the distance from the well, the pressure gradient decreases sharply. When the pressure gradient in the formation is less than the threshold pressure gradient, the heavy oil cannot flow. The corresponding area is regarded as the enrichment area of remaining oil. In addition, the pressure gradient in heavy oil reservoirs is not only related to the viscosity of crude oil but also related to the permeability of porous media. The pressure gradient in the low-permeability formation can be smaller than the threshold pressure gradient, and the pressure gradient in the high-permeability layer can be larger than the threshold pressure gradient, even at the same distance from the well.[25] This phenomenon causes water to break through quickly along the high-permeable interlayer and form the remaining oil in the rock of the low-permeability layer.[32] Therefore, for heavy oil reservoirs with water flooding, when the threshold pressure gradient of heavy oil is taken into consideration, the development scheme is appropriately selected to ensure the high enough recovery degree of the injected oil layer and reduce the remaining oil distribution area.[33]

It can be seen from the previous studies on the non-Darcy flow of heavy oil that the threshold pressure gradient is an important parameter for the flow of heavy oil in porous media, and the threshold pressure gradient plays a vital role in the distribution of remaining oil. However, there is no in-depth comparative analysis for many measuring methods of threshold pressure gradient, and there is a lack of studies considering the influence of the threshold pressure gradient on the distribution of remaining oil. Therefore, this paper takes the SZ36-1 block in a large offshore heavy oil reservoir in China as the target, selects the best measurement method of the threshold pressure gradient, and studies the influencing factors of the threshold pressure gradient and its influence on the distribution of remaining oil. Among them, the domestic large offshore heavy oil reservoir fluid is a typical Bingham fluid and its percolation law accords with the characteristics of a non-Darcy flow, and the experimental results of samples selected from this region have a certain universality to the nonlinear flow law of heavy oil. For this purpose, this paper takes the heavy oil sample of the SZ36-1 oilfield as an example to study the basic physical properties of heavy oil in this area, including rheological properties and viscosity−temperature properties, and select the optimal experimental methods based on the principle of the present methods for measuring the threshold pressure gradient. Then, the influence of the mobility of the target region on the threshold pressure gradient is researched. Finally, based on the characteristics of offshore heavy oil sandstone reservoirs, an independent numerical simulator is established to study the influence of the permeability ratio, crude oil viscosity, well pattern deployment, spacing, and fluid recovery rate on the remaining oil distribution with the threshold pressure gradient considered and not considered.

2. RESULTS AND DISCUSSION

2.1. Experimental Results and Discussion. *2.1.1. Rheological Test of Crude Oil.*

(1) Relationship between the crude oil viscosity and the shear rate

https://doi.org/10.1021/acsomega.1c04537
ACS Omega 2022, 7, 3949−3962

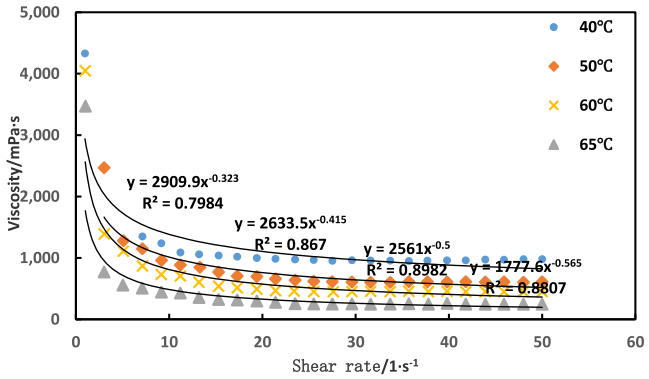

Figure 1. Relation curve between the crude oil viscosity and the shear rate in Well A7, SZ36-1 oilfield.

Table 1. Rheological Equations of Crude Oil in Well A7, SZ36-1, under Temperature Changes

temperature (°C)	rheological equation	yield stress (Pa)	Bingham viscosity (mPa·s)	R^2
40	$y = 0.9127x + 2.0881$	2.0881	912.7	0.9969
50	$y = 0.6248x + 1.2453$	1.2453	624.8	0.9993
60	$y = 0.4251x + 1.1399$	1.1399	425.1	0.9988
65	$y = 0.3355x + 1.1097$	1.1097	335.5	0.9974

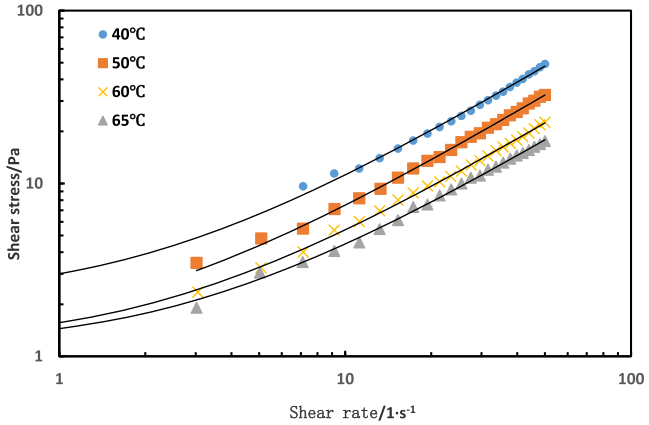

Figure 2. Rheological curve of crude oil in Well A7, SZ36-1 oilfield.

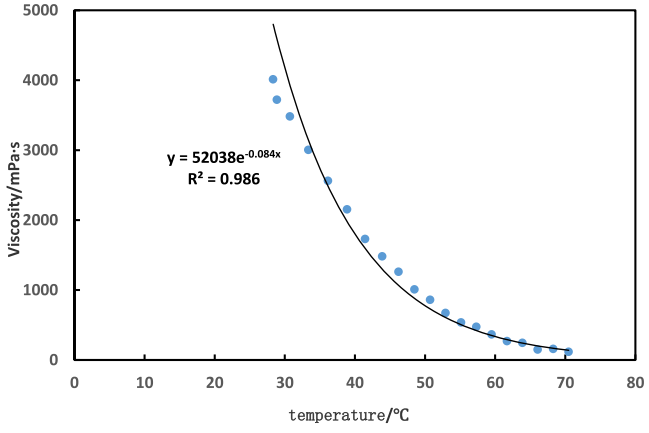

Figure 3. Viscosity−temperature curve of crude oil in Well A7, SZ36-1 oilfield.

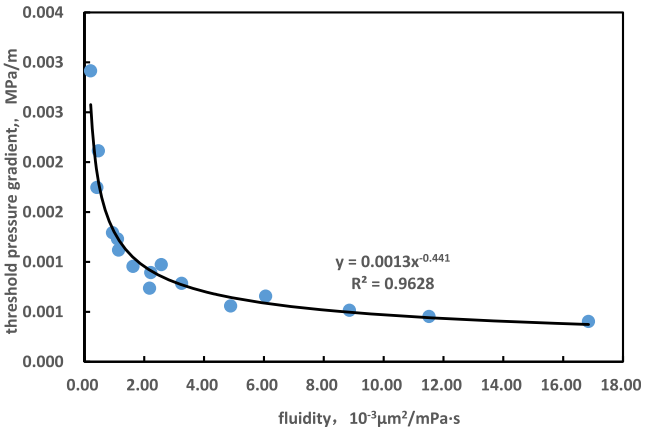

Figure 4. Relationship curve between the threshold pressure gradient and the mobility.

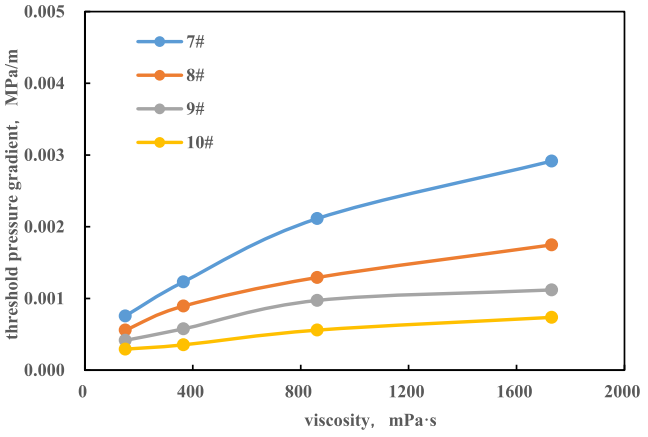

Figure 5. Relationship between the threshold pressure gradient and the viscosity of cores with different permeabilities.

Table 2. Comparison of the Threshold Pressure Gradient Measurement Methods

			threshold pressure gradient (MPa/m)		
core number	permeability (10^{-3} μm^2)	viscosity of crude (mPa·s)	MFEDP method	CE method	PCF method
1#	105.4	288.6	0.00612	0.00422	0.01235
2#	115.9	144.5	0.00526	0.00395	0.00946
3#	895.6	288.6	0.00294	0.00198	0.00755
4#	883.4	144.5	0.00198	0.00147	0.00631

It can be seen from Figure 1 that with the increase of the shear rate, the apparent viscosity of heavy oil decreases, the phenomenon named shear thinning, which is a character of non-Newtonian fluids. The viscosity of crude oil decreases sharply with the increase of the shear rate under 10 s^{-1}. The apparent viscosity of crude oil decreases slowly with the increase of the shear rate under 10 s^{-1}. When the shear rate reaches 35 s^{-1}, the apparent viscosity basically does not change with the shear rate. The reason for this phenomenon is that as the heavy oil flows, the long and thin fibers, which are disorderly and curly like long-chain molecules, are arranged along the shear direction, and the apparent viscosity decreases.[34] When the shear rate is large enough, the disorderly coiled molecules reach the maximum stretch and orientation, and, at the same time, the

https://doi.org/10.1021/acsomega.1c04537
ACS Omega 2022, 7, 3949−3962

Table 3. Experiment Results of Threshold Pressure Gradient under Different Mobilities

core number	permeability (10^{-3} μm^2)	irreducible water saturation (%)	temperature (°C)	viscosity (mPa·s)	mobility (10^{-3} μm^2/mPa·s)	threshold pressure gradient (MPa/m)
5#	406.33	19.08	40	1730.40	0.23	0.00292
			50	861.07	0.47	0.00211
			60	365.40	1.11	0.00123
			65	249.87	2.71	0.00096
6#	812.56	20.91	40	1730.40	0.47	0.00175
			50	861.07	0.94	0.00129
			60	365.40	2.22	0.00089
			65	249.87	5.42	0.00079
7#	2214.12	18.35	40	1730.40	1.28	0.00112
			50	861.07	2.57	0.00097
			60	365.40	6.06	0.00066
			65	249.87	14.77	0.00052
8#	4210.06	17.25	40	1730.40	2.43	0.00074
			50	861.07	4.89	0.00056
			60	365.40	11.52	0.00045
			65	249.87	28.09	0.00040

Table 4. Oil Recovery Situation under Different Viscosities

		zonal recovery efficiency (%)				
viscosity		layer 1	layer 2	layer 3	total recovery efficiency (%)	final moisture content (%)
considering	300	8.52	18.28	23.64	16.84	83.14
	500	6.01	13.49	18.62	12.73	75.13
not considering	300	9.15	18.72	24.81	17.57	83.22
	500	6.68	14.4	20.2	13.8	77.3

apparent viscosity reaches an equilibrium when increasing the shear rate will not change the apparent viscosity.[35,36]

(2) Yield stress of crude oil

As can be seen from Figure 2 and Table 1, crude oil from Well A7 in SZ36-1 Oilfield belongs to Bingham fluids and has yield stress. Yield stress is an important parameter of rheological properties, which reflects the plasticity of the fluid and indicates that the fluid has certain solid properties.[37] Theoretically, crude oil can only flow when the driving pressure is greater than the yield stress.[38] The influence of temperature on the yield stress is very obvious, the yield stress at high temperature is low, and with the decrease of temperature, the yield stress increases quickly. With the increase of temperature, the degree of random thermal motion of molecules is strengthened, the molecular distance increases, and the interaction between asphaltene and asphaltene (gum) is weakened. This causes more energy to form more "holes" (free volumes) inside the system, thus making it easier for the chain to move. Therefore, when micelles and micelles are connected or disassembled, the network structure is destroyed so that the internal structure of heavy oil becomes loose, the cohesion of crude oil decreases, the intramolecular friction decreases, and finally, the viscosity and yield stress decrease.[39]

(3) Influence of temperature on the rheological properties of crude oil

The trend of rheological curves in Figures 1−3 shows that the temperature has a great influence on the crude oil viscosity. At the same shear rate, the viscosity of crude oil increases with the decrease of temperature. As shown in Table 1, the rheological equation is obtained by linear fitting the relationship between the shear rate and the shear stress, in which the constant term represents the yield stress and the slope represents the plastic viscosity. As the temperature rises, the increasing random thermal motion of molecules increases the distance between molecules, which in turn weakens the interaction between asphaltenes and gums. At the same time, the continuous formation of "holes" due to the increase in the energy in the system enhances the mobility of the segment chains, and the micelles are connected or disassembled to destroy the network structure of asphaltene and colloids. As a result, the internal structure of heavy oil becomes loose, the cohesion of crude oil

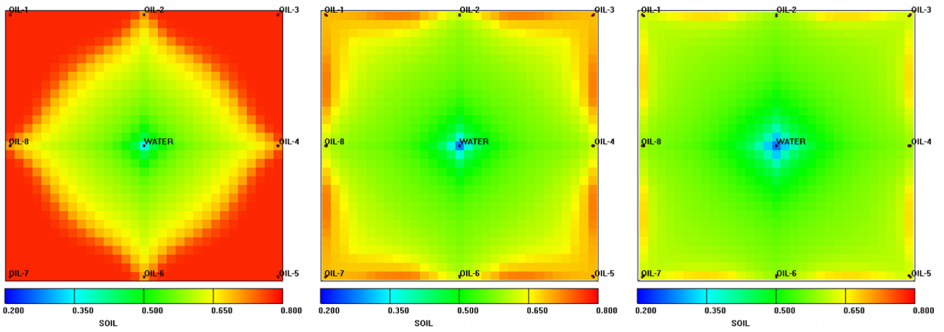

Figure 6. Distribution of remaining oil without considering the threshold pressure gradient when the crude oil viscosity is 300 mPa·s.

https://doi.org/10.1021/acsomega.1c04537
ACS Omega 2022, 7, 3949−3962

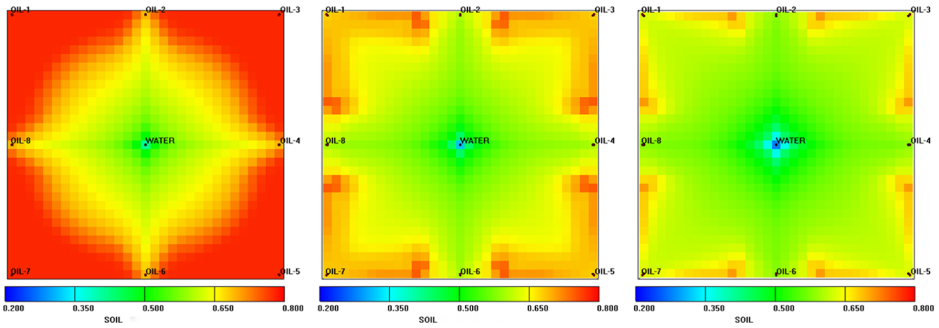

Figure 7. Distribution of remaining oil considering the threshold pressure gradient when the crude oil viscosity is 300 mPa·s.

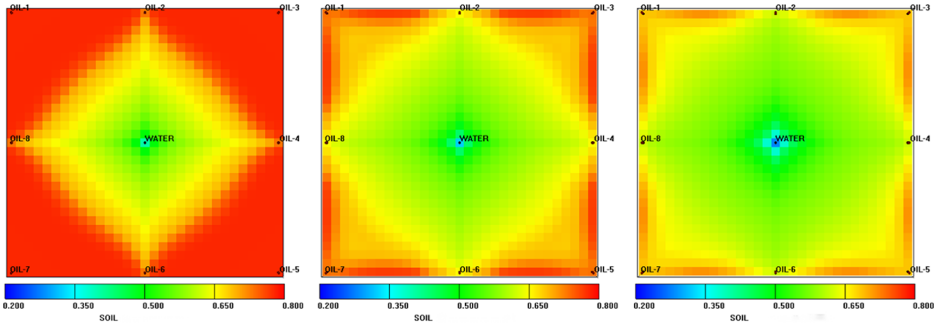

Figure 8. Distribution of remaining oil without considering the threshold pressure gradient when the crude oil viscosity is 500 mPa·s.

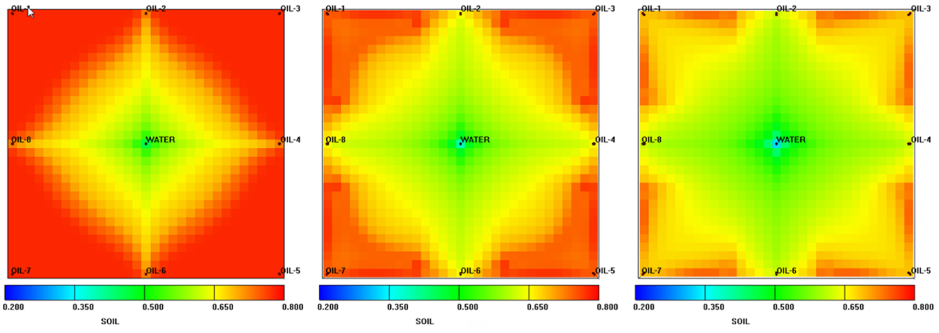

Figure 9. Distribution of remaining oil considering the threshold pressure gradient when the crude oil viscosity is 500 mPa·s.

Table 5. Oil Recovery Situation under Different Pattern Arrangements

well pattern		zonal recovery efficiency (%)			total recovery efficiency (%)	final moisture content (%)
		layer 1	layer 2	layer 3		
considering	five-point well pattern	2.71	7.14	15.40	8.42	95.56
	inverted nine-spot pattern	3.07	8.14	16.77	9.33	96.03
not considering	five-point well pattern	1.88	9.59	19.73	10.39	94.66
	inverted nine-spot pattern	3.02	9.46	20.78	11.09	95.37

decreases, and the friction between molecules decreases, so the viscosity decreases.[40]

According to the viscosity−temperature curve in Figure 5, the regression equation is in good agreement with the Arrhenius equation

$$\eta = 52{,}038 \times e^{-0.084T} \quad (1)$$

$$\eta = 1000Ae^{\Delta E/(RT)} = 1000A\ e^{BT} \quad (2)$$

where η is the viscosity of heavy oil, mPa·s; A is a constant; R is the universal gas constant; T is the thermodynamic temperature, K; ΔE is the activation energy, J/mol; and $B = \Delta E/R$ is a constant.

Derivation of eq 2 is performed to obtain eq 3

$$\frac{d\eta}{dT} = -A\ e^{B/T}B/T^2 = -B\eta/T^2 \quad (3)$$

The absolute value of $d\eta/dT$ reflects the rate of change of viscosity with temperature, and $B\eta$ in eq 3 is proportional to the slope of the viscosity−temperature curve at a certain temperature, which shows the rate of change of viscosity when the temperature rises or falls. The sharper the slope, the more sensitive the viscosity is to the temperature.[41]

https://doi.org/10.1021/acsomega.1c04537
ACS Omega 2022, 7, 3949−3962

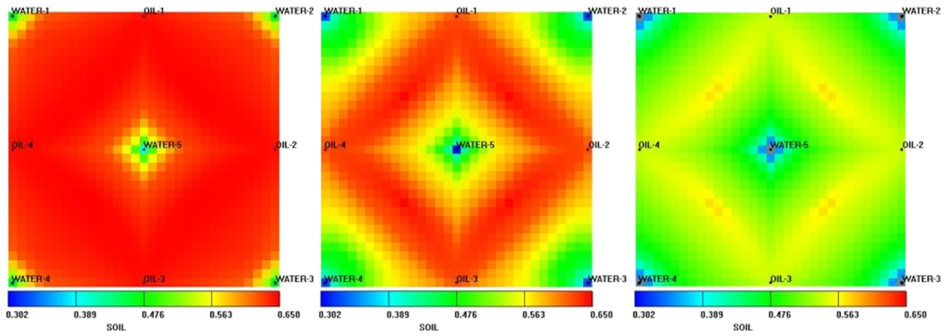

Figure 10. Distribution of remaining oil under the five-point well pattern without considering the threshold pressure gradient.

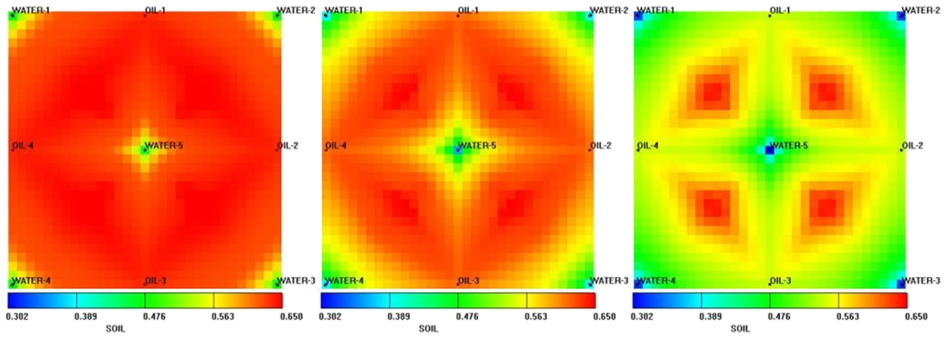

Figure 11. Distribution of remaining oil under the five-point well pattern considering the threshold pressure gradient.

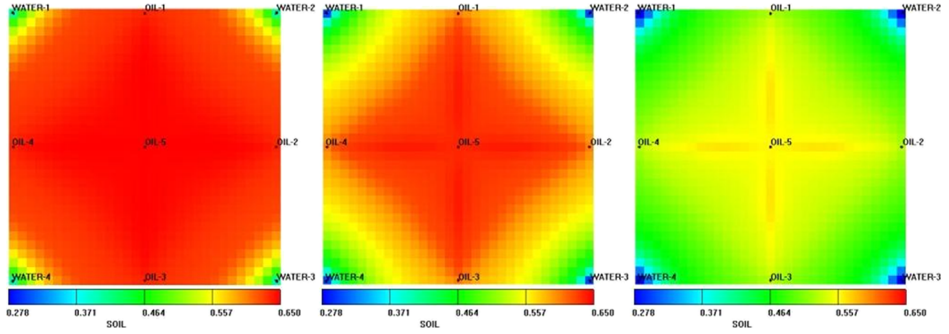

Figure 12. Distribution of remaining oil under the inverted nine-spot pattern without considering the threshold pressure gradient.

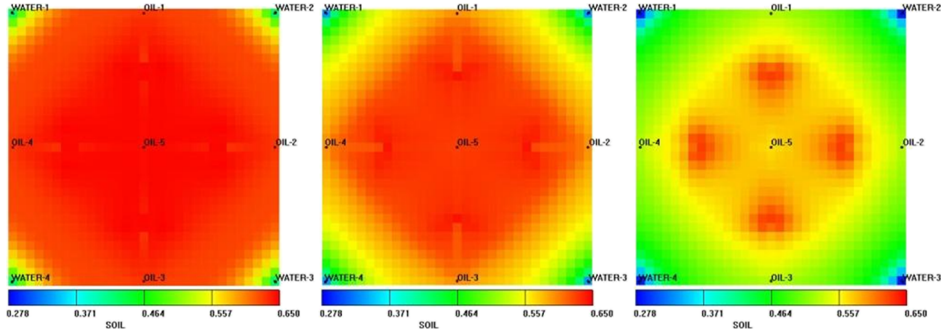

Figure 13. Distribution of remaining oil under the inverted nine-spot pattern considering the threshold pressure gradient.

2.1.2. Experiments on Threshold Pressure Gradient.

(1) Comparison of threshold pressure gradient measurement methods

The microflow-established differential pressure method (MFEDP) displaces a fluid with a small flow rate and gradually establishes the pressure difference at the inlet end of the core. It is considered that the instantaneous pressure of the fluid flow is the threshold pressure. The threshold pressure gradient measured by this method can approximately represent the real threshold pressure gradient of the core. The PCF method fits the percolation curve obtained from the experiment, and the constant term in the fitting formula is the threshold pressure gradient. According to Table 2, the value of the threshold pressure gradient obtained by the PCF method is 1.79 to 3.19

https://doi.org/10.1021/acsomega.1c04537
ACS Omega 2022, 7, 3949−3962

Table 6. Crude Oil Recovery under Different Well Spacing Conditions

		zonal recovery efficiency (%)				
well spacing (m)		layer 1	layer 2	layer 3	total recovery efficiency (%)	final moisture content (%)
considering	300	8.89	19.44	24.38	17.76	91.08
	500	6.15	13.87	19.03	13.04	69.79
not considering	300	8.69	16.67	26.82	17.42	88.96
	500	6.93	15.01	20.86	14.28	72.59

times that obtained by the MFEDP method. The threshold pressure gradient obtained by formula fitting is closely related to the selection of the fluid flow velocity in the percolation curve. In the process of actually measuring the percolation curve, it is often affected by the equipment accuracy and the experimental cycle. Therefore, it is difficult to obtain the percolation curve under a minimum fluid flow velocity, and the larger the selected fluid flow velocity is, the larger the obtained threshold pressure gradient. Using the law of connected vessels, the CE method considers that when the fluid in the core does not flow, the height difference of the liquid column at both ends of the core is the threshold pressure. According to Table 2, the value of the threshold pressure gradient obtained by the CE method is 0.67 to 0.75 times that obtained by the MFEDP method. The measurement principle of the CE method is the pressure difference between the two ends of the core when the fluid goes from a flowing state to a static state. When the heavy oil is in a static state, the internal structure has a certain strength. As the pressure gradually rises, the internal structure begins to deform until the ultimate pressure of structural failure is reached and the heavy oil begins to flow. Once the structure of heavy oil is destroyed, it is difficult to restore to its original state.[41] However, the threshold pressure gradient of the heavy oil whose structure has been damaged is measured by the principle of the connector. Therefore, the pressure gradient measured by the CE method is less than the real threshold pressure gradient.

(2) Experiments on the influence factor of threshold pressure gradient

It can be seen in Figure 4 that when the mobility is small, the threshold pressure gradient decreases rapidly with the increase of mobility, while the threshold pressure gradient decreases slowly with the continuous increase of mobility, and a power function is used to fit. The cause of this phenomenon is that the colloid, asphaltene, and polymer hydrocarbon content in the crude oil decrease continuously with the decrease of viscosity, leading to smaller intermolecular forces, and with the increase of permeability, the intermolecular forces decline faster, resulting in the decrease of threshold pressure gradient with the increase of mobility (Table 3).[19,23,41−47]

2.2. Influence of Threshold Pressure Gradient on Remaining Oil Distribution. *2.2.1. Viscosity of Crude Oil.* By comparing the simulation results, it can be concluded that with the increase of viscosity, the percolating resistance increases, the water-flooding development rate becomes smaller, the remaining oil increases, and the recovery efficiency of each layer decreases; for the same oil viscosity, considering the threshold pressure gradient, the more the remaining oil, the higher the oil viscosity is. Considering the threshold pressure gradient, the remaining oil in the second layer is more concentrated at 1/4 of the distance to the side well and the corner well, showing the shape of a wedge. However, without considering the threshold pressure gradient, the remaining oil shows a straight-line distribution along the corner wells. The results are shown in Table 4 and Figures 6−9.

2.2.2. Pattern Arrangement. By comparing the simulation results, it can be concluded that the remaining oil distribution mode is different for various well patterns. Under the five-point well pattern, the remaining oil is distributed between the injection wells. However, for the inverted nine-spot pattern, the remaining oil is mainly distributed near the oil wells. Considering the threshold pressure gradient, the remaining oil is mostly aggregated between injection wells under the five-point well pattern. However, for the inverse nine-spot well pattern, the remaining oil is mainly distributed near the oil well, especially at a 1/4 distance from the side well and the corner well, and the remaining oil is more concentrated. The results are shown in Table 5 and Figures 10−13.

2.2.3. Well Spacing. It can be seen from the simulation results that well spacing has a great influence on the distribution of remaining oil; the larger the well spacing, the more the remaining oil is, which is distributed mostly between oil wells. When considering the threshold pressure gradient, the remaining oil is mostly enriched near the well, but to a certain extent, it reduces the imbalance distribution of remaining oil between layers, especially in the case of an oilfield with a large well spacing, which can help alleviate uneven development conditions; the results are shown in Table 6 and Figures 14−17.

2.2.4. Fluid Recovery Rate. Comparing the simulation results, it can be concluded that the remaining oil distribution is greatly affected by the fluid production rate; the greater the fluid recovery rate, the smaller the remaining oil saturation. At the same fluid recovery rate, the more the remaining oil, the

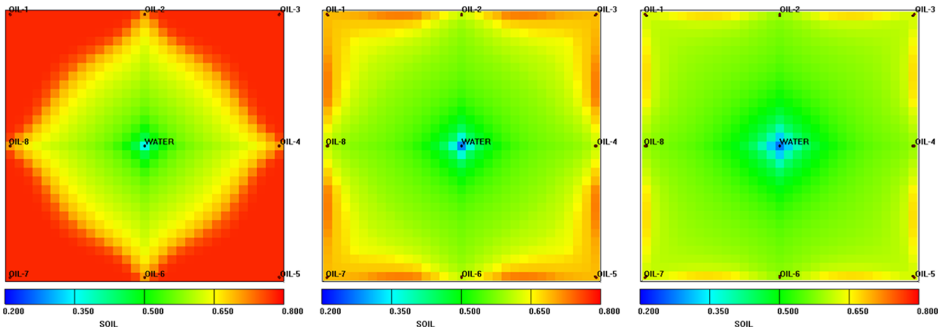

Figure 14. Distribution of remaining oil without considering the threshold pressure gradient when the well spacing is 400 m.

https://doi.org/10.1021/acsomega.1c04537
ACS Omega 2022, 7, 3949−3962

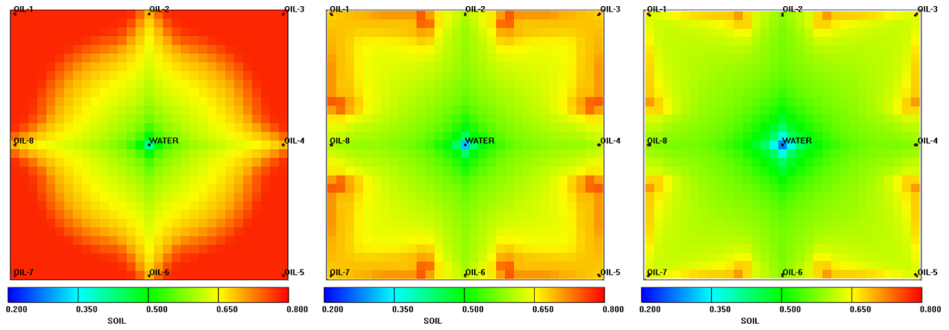

Figure 15. Distribution of remaining oil considering the threshold pressure gradient when the well spacing is 400 m.

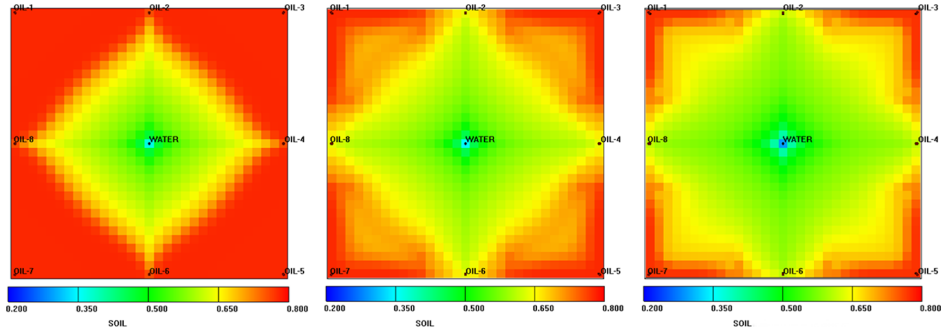

Figure 16. Distribution of remaining oil without considering the threshold pressure gradient when the well spacing is 500 m.

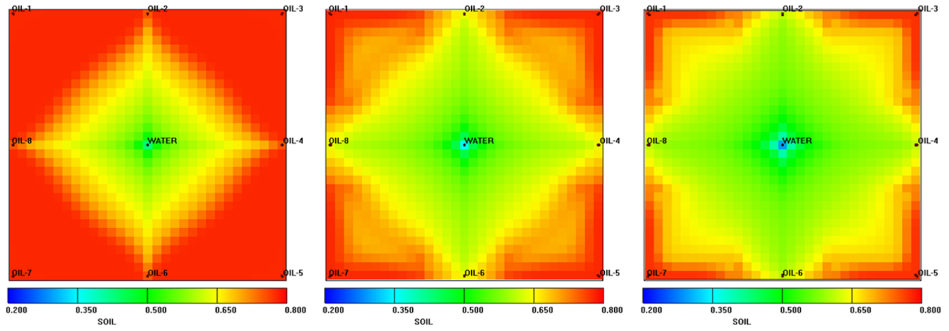

Figure 17. Distribution of remaining oil considering the threshold pressure gradient when the well spacing is 500 m.

Table 7. Crude Oil Recovery at Different Fluid Recovery Rates

fluid recovery rate		zonal recovery efficiency (%)			total recovery efficiency (%)	final moisture content (%)
		layer 1	layer 2	layer 3		
considering	1%	1.71	4.35	6.43	4.16	11.64
	3%	6.04	14.01	19.63	13.25	64.57
not considering	1%	1.80	3.86	6.74	4.13	16.23
	3%	6.67	14.89	21.01	14.20	68.18

higher the fluid recovery rate considering the pressure gradient. The oil−water front advances toward the well in the shape of a star when the fluid recovery rate is 1% considering the threshold pressure gradient and in the shape of a rhomboid without considering the threshold pressure gradient. The rhomboid area is significantly larger than the star area, so the remaining oil is more concentrated. The results are shown in Table 7 and Figures 18−21.

3. CONCLUSIONS

In this paper, the rheological properties of heavy oil in the SZ36-1 oilfield were studied based on the experiments of heavy oil threshold pressure gradient and the numerical simulation of its effect on the distribution of remaining oil. The relationship between the threshold pressure gradient and mobility was studied with an accurate measurement method, as well as the influence of threshold pressure gradient on the distribution of remaining oil. The main conclusions are as follows:

(1) The fluids in the SZ36-1 oilfield have the rheological characteristics of Bingham fluids: ① the viscosity decreases sharply with the increase of the shear rate when the shear rate is less than 10 s^{-1}. When the shear rate is between 10 and 40 s^{-1}, the apparent viscosity decreases slowly with the increase of the shear rate. When the shear

https://doi.org/10.1021/acsomega.1c04537
ACS Omega 2022, 7, 3949−3962

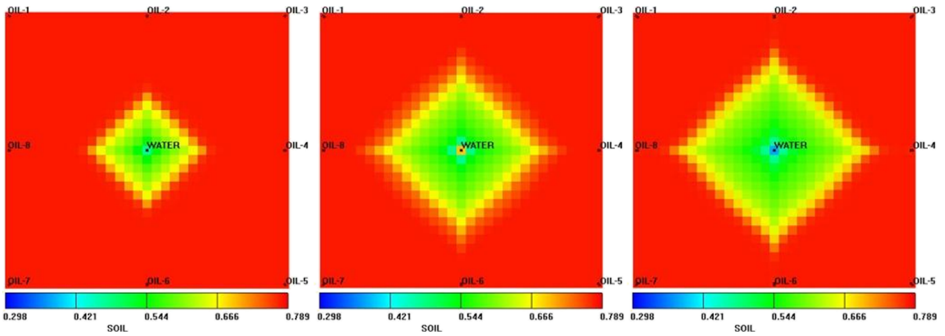

Figure 18. Distribution of remaining oil not considering threshold pressure gradient when the fluid recovery rate is 1%.

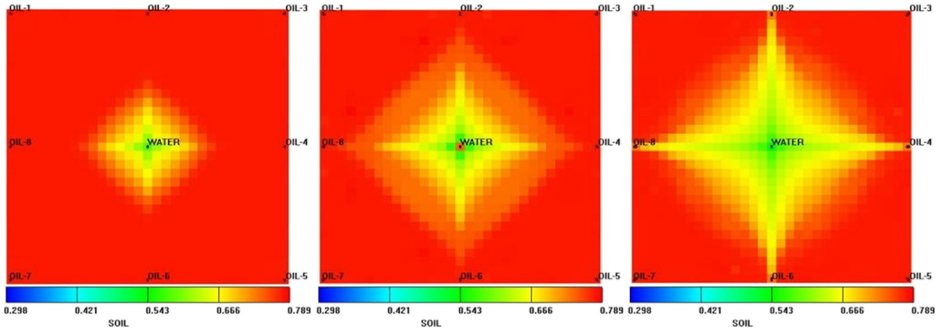

Figure 19. Distribution of remaining oil considering the threshold pressure gradient when the fluid recovery rate is 1%.

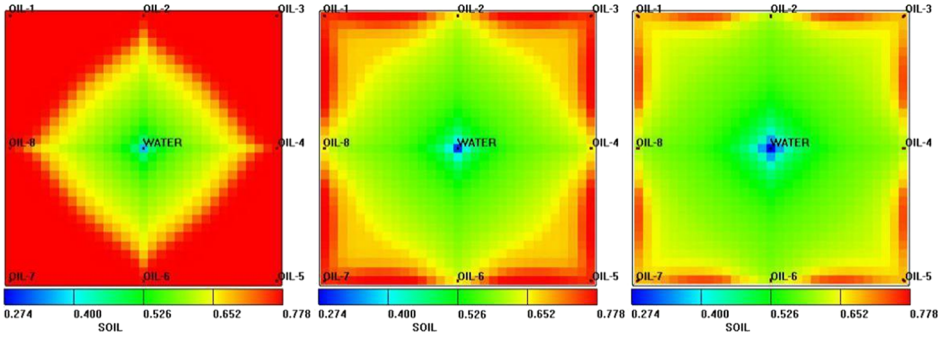

Figure 20. Distribution of remaining oil not considering threshold pressure gradient when the fluid recovery rate is 3%.

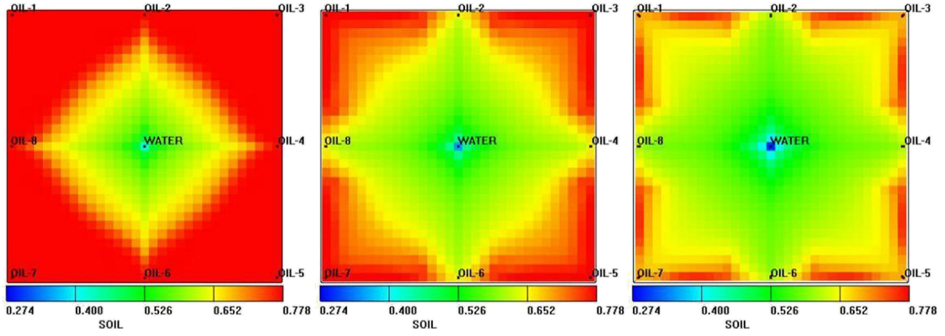

Figure 21. Distribution of remaining oil considering the threshold pressure gradient when the fluid recovery rate is 3%.

rate is below 40 s^{-1}, the apparent viscosity does not change with the shear rate or fluid flow velocity. ② At the same shear rate, the viscosity of heavy oil increases with the decrease of temperature, and the increase rate of viscosity is faster. The lower the temperature, the larger the slope of the rheological curve of crude oil, and the more obvious the non-Newtonian characteristics. ③ The fluid has certain solid characteristics; only when the force is greater than the yield value, the fluid can flow.

(2) In the three measurement methods of threshold pressure gradient, the MFEDP method is optimized to study the effect of mobility on the threshold pressure gradient. The result shows that with the increase of mobility, the threshold pressure gradient descends faster under small

https://doi.org/10.1021/acsomega.1c04537
ACS Omega 2022, 7, 3949−3962

Table 8. Four Components of Crude Oil from Well A7 of SZ36-1 Oilfield

asphaltene content (%)	colloid content (%)	aromatic hydrocarbon content (%)	saturated hydrocarbon content (%)	viscosity (30 °C) (mPa·s)	relative density
7.78	21.66	29.5	41.06	3481	0.9012

Table 9. Ion Content of Brine in the SZ36-1 Oilfield

		ion content (mg/L)							
pH value	density (g/cm^3)	Ca^{2+}	Mg^{2+}	$K^+ + Na^+$	Cl^-	SO_4^{2-}	HCO_3^-	total salinity (mg/L)	water type
7.13	1.042	241.35	402.56	10,394.61	11,336.29	680.79	2837.84	22,940	$CaCl_2$

mobility, and then the descent rate slows down with the continuous increase of mobility. The threshold pressure gradient and mobility have a power function relation.

(3) A self-developed numerical simulator was used to simulate the well group model, and it was found that when considering the threshold pressure gradient of heavy oil, an additional percolating resistance would be generated in the process of water flooding, which intensified the uneven distribution of remaining oil and led to more enrichment of remaining oil. It can be seen from the simulation results that the total recovery degree after considering the threshold pressure gradient is 0.75−1.97% lower than that without considering the threshold pressure gradient, and the final water cut is 2.8−4.59% lower. The main influence of additional percolating resistance is reflected in three aspects: ① acceleration of the formation of the minimum percolating resistance channel, along which most injected water advances so that the spread range is greatly reduced; ② aggravation of the water−oil mobility difference, leading to a more serious water-phase fingering phenomenon and a non-piston phenomenon in the displacement process, so the oil displacement efficiency is greatly reduced; and ③ intensification of the difference in the interlayer percolating resistance and further intensification of the interlayer contradiction.

4. EXPERIMENTAL AND NUMERICAL SECTION

4.1. Experiments. *4.1.1. Materials and Parameters.* Crude oil sample: the dehydrated crude oil from the wellhead of Well A7 of SZ36-1 oilfield was selected, and its components are shown in Table 8.

Table 10. Basic Parameters of Cores

core number	length (cm)	diameter (cm)	porosity (%)	gas permeability ($\times 10^{-3}$ μm^2)	experiment item
1#	5.658	2.481	34.58	105.4	comparative measurement methods of the threshold pressure gradient
2#	5.651	2.485	32.16	115.9	
3#	5.516	2.489	34.57	895.6	
4#	5.628	2.485	32.03	883.4	
5#	10.22	2.52	34.84	406.33	effect of mobility on the threshold pressure gradient
6#	10.21	2.52	24.32	812.56	
7#	10.21	2.52	30.49	2214.12	
8#	10.21	2.52	33.69	4210.06	

Table 11. Experimental Conditions

method	experimental temperature (°C)	process of displacement	seepage velocity (mL/min)
MFEDP method (Wang et al., 2013)	30	constant speed	0.003
PCF method (Tian et al., 2009)	30	constant speed	0.05
CE method (Song et al., 1999)	30	constant speed	0.01−5.00

Figure 22. MCR301-type rheometer.

Experimental water: according to the ion content of brine in the SZ36-1 oilfield, simulated formation water was configured, filtered, and vacuumed at the lab; the formation water ion content of the SZ36-1 oilfield is shown in Table 9.

Experimental cores: artificial sandstone cores with permeability similar to that of SZ36-1 were used to conduct threshold pressure gradient experiments. The basic core parameters are shown in Table 10.

Experimental conditions: the experimental conditions are shown in Table 11.

4.1.2. Equipment and Flow Chart. The rheological test equipment of crude oil is an MCR301-type rheometer (Figure 22).

As shown in Figure 23, the displacement range of the ISCO pump is 0−60 mL/min (±0.001 mL/min), the pressure is 0−70 MPa (±0.001 MPa), the temperature range is room temperature−150 °C (±0.1 °C), and the pressure range of the core inlet tube is 0.00005−0.01 MPa.

4.1.3. Experimental Methods.

(1) Crude oil rheological test

The viscosity of the crude oil from Well A7 at different shear rates (1−50 s^{-1}) and the rheological characteristic curves at different temperatures (40, 50, 60, 65 °C) were measured with the Anton Paar MCR301-type rheometer.

(2) Experiment on the threshold pressure gradient

https://doi.org/10.1021/acsomega.1c04537
ACS Omega 2022, 7, 3949−3962

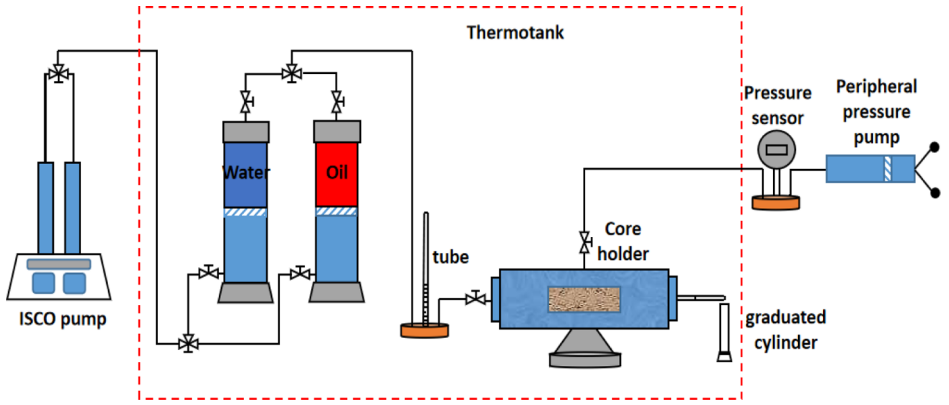

Figure 23. Schematic diagram of measuring the threshold pressure gradient.

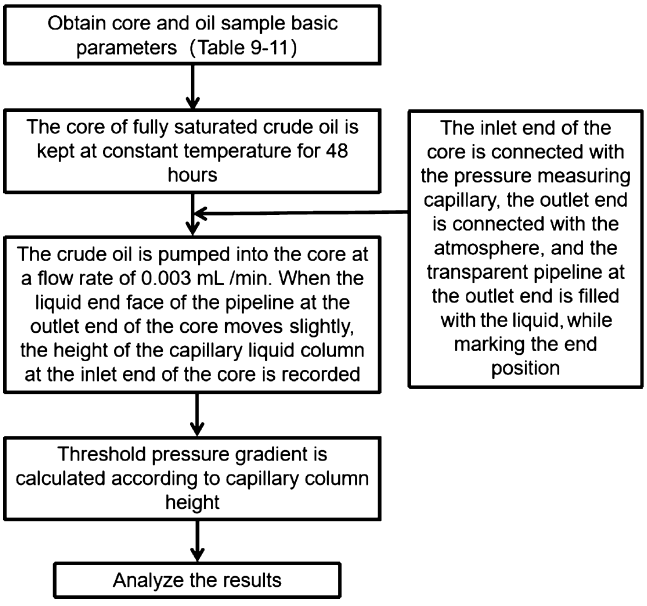

Figure 24. MFEDP method flow chart.

A Threshold pressure gradient measurement methods

During the experiment, the same permeability core and the same viscosity crude oil were selected. The MFEDP method, CE method, and PCF are used to compare the measuring result for the optimal measurement method. In addition, in order to avoid the influence of irreducible water saturation on the results, the experiment was carried out with a completely crude oil-saturated core. The basic parameters are shown in Table 11.

MFEDP method:[48,49] The fluid is displaced with a flow rate of 0.003 mL/min, and the inlet pressure is slowly increased to observe the outlet liquid situation. When the outlet liquid starts moving, the corresponding inlet pressure is regarded as the threshold pressure (in order to get a more accurate measurement of the pressure difference, the liquid height is used as a pressure differential gauge) and thus the threshold pressure gradient is calculated (Figure 24).

CE method:[50] The fluid is displaced at a flow rate of 0.05 mL/min until the liquid surface at the outlet begins to flow, then the liquid intake switch is closed, the liquid height is recorded at different times until it stays stable, and the threshold pressure and the threshold pressure gradient of the core are calculated (Figure 26).

PCF method:[23] Based on the pressure−flow curve, by changing the pressure difference at both ends of the core and measuring the flow velocity of the fluid through the core, the pressure gradient−seepage velocity curve is obtained, and then using the intercept of the curve on the coordinate axis, the threshold pressure gradient of the core is obtained (Figure 25).

B Factors influencing the threshold pressure gradient

Four kinds of cores with various permeabilities were selected to carry out threshold pressure gradient experiments under different mobilities. The experimental temperature was set to 40, 50, 60, and 65 °C to change the viscosity of crude. The basic core parameters are shown in Table 11.

4.2. Numerical Modeling. *4.2.1. Flow Equation.* To realize the numerical simulation of water flooding heavy oil, the threshold pressure gradient is considered not only in the mesh equation but also in the well-grid flow equation to ensure the well-posedness of the numerical model, or contradiction will be produced in the well-grid flow and grid−grid flow. Xi et al. described and derived a well-grid mathematical model for nonlinear flow,[17] and the main theoretical formula is as follows

$$Q_l = \begin{cases} 0 & |\bar{\Phi}_l - \Phi_{lwf}| < \frac{2}{3} r_e G \\ \dfrac{2\pi K K_{rl} h}{\mu_l} \dfrac{\bar{\Phi}_l - \Phi_{lwf} \pm \frac{2}{3} r_e G}{\left(\ln \frac{r_e}{r_w} - \frac{1}{2}\right)} & |\bar{\Phi}_l - \Phi_{lwf}| \geq \frac{2}{3} r_e G \end{cases} \quad (4)$$

Equation 4 is the well-grid equation for a nonlinear flow, in which a negative sign is taken for the producing well and a positive sign is taken for the injection well. In the case of water flooding heavy oil, when l = g, w, G in the above equation should be 0, meaning a Darcy flow. When l = o, G is not 0. In this case, the oil phase has a nonlinear flow and varies with mobility.

4.2.2. Establishment of the Mechanism Model. At present, there is no keyword describing the threshold pressure gradient in commercial software, so it can only be simulated by equivalent methods. ECLIPSE uses the keyword THPRES to set the equivalent threshold pressure, which represents the minimum pressure difference at which the fluid between adjacent balance zones can seep, then the equivalent threshold pressure gradient is approximated. In ECLIPSE, a "circular convolution" arrangement is used to partition the grid, which requires a lot of work, increases the amount of calculation, and deteriorates the convergence. Since the threshold pressure is set to be equivalent to the threshold pressure in Eclipse, the propagation direction of

https://doi.org/10.1021/acsomega.1c04537
ACS Omega 2022, 7, 3949−3962

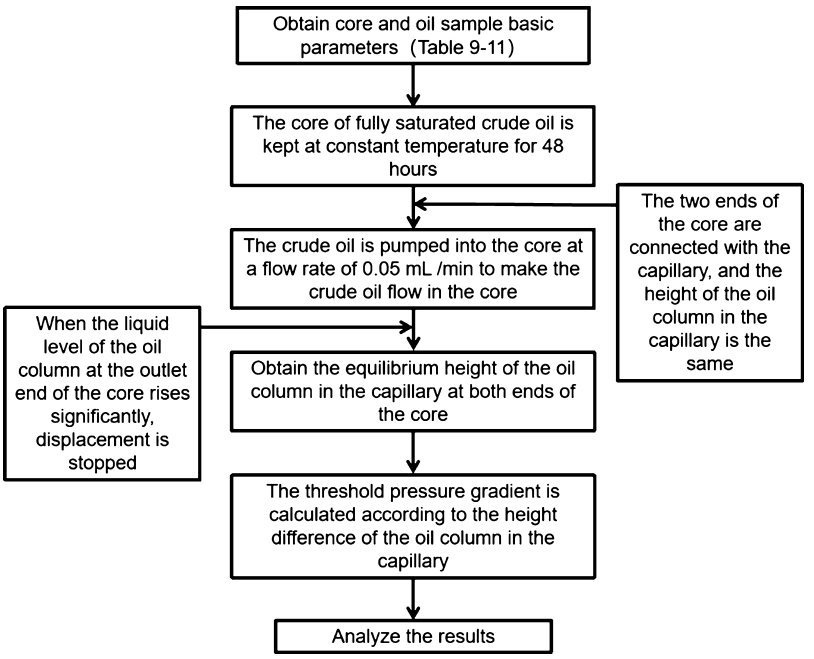

Figure 25. CE method flow chart.

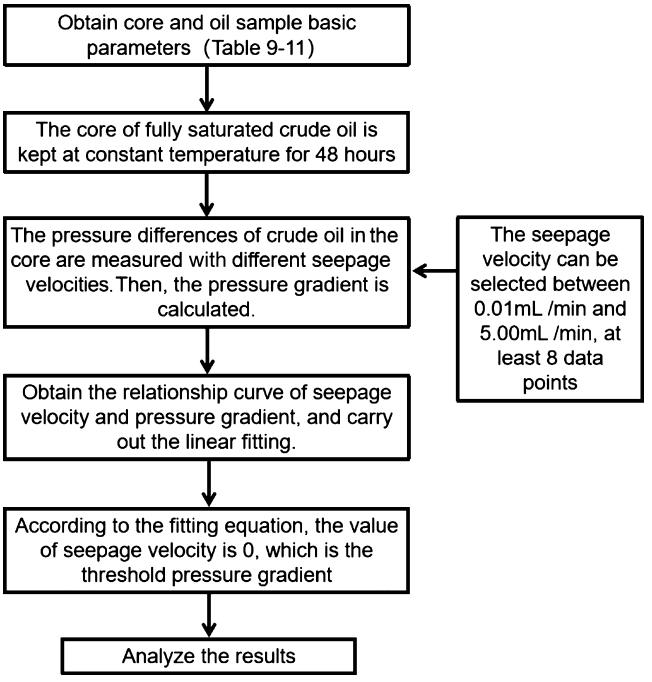

Figure 26. PCF method flow chart.

Table 12. Values of Design Factors and Permeability

permeability setting	permeability ratio of 3
1	300
2	600
3	900

pressure is uniform and has no selectivity. In CMG, the keyword PTHRESHI is used to set the start pressure gradient, which is simpler than the ECLIPSE setting. It is equivalent to a "one-time switch". Once the displacement pressure gradient is higher than the threshold pressure gradient, the grids can circulate. When the gradient is lower than the threshold pressure gradient, no further inspection is required, and the grids still maintain circulation, which does not match the actual situation. However, in oilfield production, the pressure difference is very large, but the pressure gradient along some streamline may be very small, so the fluid cannot flow and the pressure cannot spread. Therefore, the pressure wave in the injection well propagates in the direction where the fluid flow path is so short that the displacement pressure gradient is greater than the threshold pressure gradient. Therefore, considering the threshold pressure gradient (not threshold pressure), the range of water injection well pressure is much smaller than that of the threshold pressure.

In this article, a self-developed NRSNL numerical simulator is set to simulate the threshold pressure gradient through the keyword non-newton-fluid. In addition, for the degradation test and the SPE test of the self-developed NRSNL numerical simulator, we refer to the article of Xi.[18,50] The degenerated NRSNL numerical simulator is basically consistent with the formation pressure curve, water cut, daily oil production, and formation pressure calculated by ECLIPSE and CMG. Therefore, the self-developed NRSNL numerical simulator is reasonable.

Based on the characteristics of the offshore heavy oil sandstone reservoir, the research factors of the model include the viscosity of crude oil, well pattern deployment, well spacing, and fluid recovery rate, and so forth. The values of design factors and permeability are shown in Table 12, and 13 shows the basic parameters of the model.

Viscosity of crude oil: A positive rhythm model with a well spacing of 400 m, a longitudinal interlayer permeability ratio of 3, an oil recovery rate of 3%, a formation thickness of 10 m, and oil viscosities of 300 and 500 mPa·s (the parameter setting is shown in Table 13).

Pattern arrangement: A five-point method and a reverse nine-point method are selected. A small layer thickness of 10 m, a longitudinal interlayer permeability ratio of 3, a viscosity of 300 mPa·s, and an oil recovery rate of 3% (model parameters are shown in Table 13) are used.

https://doi.org/10.1021/acsomega.1c04537
ACS Omega 2022, 7, 3949−3962

Table 13. Basic Parameters of the Model

heterogeneity of permeability (permeability ratio)	well spacing (m)	viscosity (mPa·s)	thickness of a single layer (m)	well pattern	oil production rate (%)	rhythm	vertical/horizontal
3	400	300	10	Inverted nine-spot injection pattern	3%	Positive rhythm	Vertical well

Well spacing: Three models (parameters are shown in Table 13) with a single layer thickness of 10 m, a vertical interlayer permeability ratio of 3, a viscosity of 300 mPa·s, an oil recovery rate of 3%, and well spacings of 300 and 500 m were selected for comparison.

Fluid recovery rate: The fluid recovery rate is set as 1 and 3% (the parameter setting is shown in Table 13) for simulation.

AUTHOR INFORMATION

Corresponding Authors

Yuetian Liu − *China University of Petroleum at Beijing, 102249 Beijing, China;* orcid.org/0000-0002-9431-1031; Email: lyt51@163.com

Gaoming Yu − *Yangtze University, 430100 Wuhan, Hubei, China*; Email: ygm1210@vip.sina.com

Authors

Wenli Ke − *China University of Petroleum at Beijing, 102249 Beijing, China; Yangtze University, 430100 Wuhan, Hubei, China;* orcid.org/0000-0002-6323-9372

Xu Zhao − *Exploration and Development Research Institute of Sinopec Jianghan Oilfield Company, 434023 Wuhan, Hubei, China*

Jie Wang − *Yangtze University, 430100 Wuhan, Hubei, China;* orcid.org/0000-0001-8279-741X

Complete contact information is available at: https://pubs.acs.org/10.1021/acsomega.1c04537

Notes

The authors declare no competing financial interest.

ACKNOWLEDGMENTS

This work was financially supported by the National Science and Technology Major Projects of China (2016ZX05025-001-005).

REFERENCES

(1) Basak, P. Non-Darcy flow and its implications to seepage problem. *J. Irrig. Drain. Div., Am. Soc. Civ. Eng.* **1977**, *103*, 459.

(2) Kong, X. Y. *Advanced Mechanics of Fluid Flow in Porous Media*, 3rd ed.; University of Science and Technology of China Press, Academic Press: Hefei, 2010; pp 202−204.

(3) Xu, H.; Qin, Q. Study on water flooding characteristics and remaining oil distribution in heavy oil reservoir development. *Sci. Technol.* **2008**, *30*, 89−92.

(4) Thomas, L. K.; Katz, D. L.; Tek, M. R. Threshold pressure phenomena in porous media. *SPEJ* **1968**, *8*, 174−184.

(5) Boronin, S. A.; Osiptsov, A. A.; Desroches, J. Displacement of yield-stress fluids in a fracture. *PCH, PhysicoChem. Hydrodyn.* **2015**, *76*, 47−63.

(6) Ma, G. h. *The Relationship between Molecular Structure of Heavy Oil Composition and Viscosity−Temperature Property*; College of Chemical Engineering China University of Petroleum (East China), 2015.

(7) Rodríguez de Castro, A.; Omari, A.; Ahmadi-Sénichault, A.; Savin, S.; Madariaga, L. F. Characterizing porous media with the yield stress fluids porosimetry method. *Transp. Porous Media* **2016**, *114*, 213.

(8) Al-Fariss, T.; Pinder, K. L. Flow through porous media of a shear-thinning liquid with yield stress. *Can. J. Chem. Eng.* **2010**, *65*, 391−405.

(9) Li, C. X. *Oil Rheology*, 1st ed.; China University of Petroleum Press, Academic Press: Shandong, 2007; pp 117−123.

(10) Wang, C. Y. *Abnormal Oil*, 1st ed.; Petroleum Industry Press, Academic Press: Beijing, 1975; pp 55−61.

(11) Sun, J. F. *Research and Application on the Heavy Oil Flow Mode*, 1st ed.; China University of Ceosciences, Academic Press: Beijing, 2012; pp 30−35.

(12) Holenberg, Y.; Lavrenteva, O. M.; Liberzon, A.; Shavit, U.; Nir, A. PTV and PIV study of the motion of viscous drops in yield stress material. *J. Non-Newtonian Fluid Mech.* **2013**, *193*, 129−143.

(13) Picchi, D.; Barmak, I.; Ullmann, A.; Brauner, N. Stability of stratified two-phase channel flows of Newtonian/non-Newtonian shear-thinning fluids. *PCH, PhysicoChem. Hydrodyn.* **2018**, *99*, 111.

(14) Chen, M.; Rossen, W.; Yortsos, Y. C. The flow and displacement in porous media of fluids with yield stress. *Chem. Eng. Sci.: X* **2005**, *60*, 4183−4202.

(15) Wang, S.; Huang, Y.; Civan, F. Experimental and theoretical investigation of the Zaoyuan fifield heavy oil flow through porous media. *J. Pet. Sci. Eng.* **2006**, *50*, 83−101.

(16) Lyu, S.; Taghavi, S. M. Efficient Fluid-Fluid Displacement of Yield Stress Fluids in Axially Rotating Pipes. *38th International Conference on Ocean, Offshore and Arctic Engineering OMAE 2019 June 9−14, 2019, Glasgow, UK*, 2019.

(17) Tian, J.; Xu, J.-f.; Song, L. The Method of Characterization and Physical Simulation of TPG for Ordinary Heavy Oil. *Xinan Shiyou Daxue Xuebao* **2009**, *31*, 158−162.

(18) Song, F. Q.; Liu, C. Q. Simple indoor measurement of threshold pressure gradient. *Low Permeability Oil & Gas Field* **1999**, *004*, 48−50.

(19) Lu, C.-y.; Wang, J.; Sun, Z. G. An Experimental Study on threshold Pressure Gradient of Fluids Flow in Low Permeability Sandstone Porous Media. *Adv. Pet. Explor. Dev.* **2002**, *29*, 86−89.

(20) Tan, L. J.; Jia, Y. L.; Feng, X. Study on the threshold Pressure Gradient for the Low Velocity Non-Darcy Flow. *Well Testing* **2000**, *9*, 5−7.

(21) Li, A. F.; Zhang, S. H.; Liu, M.; Wang, W. G.; Zhang, L. A New Method of Measuring threshold Pressure for Low Permeability Reservoir. *Zhongguo Shiyou Daxue Xuebao, Ziran Kexueban* **2008**, *32*, 68−71.

(22) Xin, X. K. Study of Numerical Simulation with Water Flooding Heavy Oil Reservoir Based on Nonlinear Seepage. Master's Thesis, Yangtze University, 2013.

(23) Xin, X.; Li, Y.; Yu, G.; Wang, W.; Zhang, Z.; Zhang, M.; Ke, W.; Kong, D.; Wu, K.; Chen, Z. Non-Newtonian Flow Characteristics of Heavy Oil in the Bohai Bay Oilfield: Experimental and Simulation Studies. *Energies* **2017**, *10*, 1698.

(24) Cheng, S.; Zhang, D. Type Curve Method of Well Test Data for Non-Darcy Flow at Low Velocity. *Adv. Pet. Explor. Dev.* **1996**, *23*, 50−53.

(25) Prada, A.; Civan, F. Modification of Darcy's law for the threshold pressure gradient. *J. Pet. Sci. Eng.* **1999**, *22*, 237−240.

(26) Dmitriev, M. N.; Kadet, V. V. Generalized Darcy's Law and the Structure of the Phase and Relative Phase Permeabilities for Two-Phase Flows through Anisotropic Porous Media. *Fluid Dyn.* **2003**, *38*, 284−292.

(27) Han, H. B. Physical Simulation and Numerical Simulation Method Considering Threshold Pressure Gradient in Ultra-low Permeability Reservoir. *SPEJ* **2013**, *8*, 174.

(28) Balhoff, M.; Sanchez-Rivera, D.; Kwok, A.; Mehmani, Y.; Prodanović, M. Numerical Algorithms for Network Modeling of Yield Stress and other Non-Newtonian Fluids in Porous Media. *Transp. Porous Media* **2012**, *93*, 363−379.

(29) Yazdchi, K.; Luding, S. Upscaling and Microstructural Analysis of the Flow-structure Relation Perpendicular to Random, Parallel Fiber Arrays. *Chem. Eng. Sci.* **2013**, *98*, 173−185.
(30) Zhao, G. Z. Establishment of The High-efficieny Solver for Distributed Parallel Reservoir Simulation. *Daqing Shiyou Dizhi Yu Kaifa* **2016**, *35*, 53−57.
(31) Kurimoto, R.; Nakazawa, K.; Minagawa, H.; Yasuda, T. Prediction models of void fraction and pressure drop for gas-liquid slug flow in microchannels. *Exp. Therm. Fluid Sci.* **2017**, *88*, 124−133.
(32) Huang, Y.; Yang, Z.; He, Y. An overview on nonlinear porous flow in low permeability porous media. *Theor. Appl. Mech. Lett.* **2013**, *3*, 8.
(33) Flock, D. L. The theology of heavy crude oils and their emulsions. *Pet. Soc. CIM* **1983**, *22*, 38−52.
(34) Khatyr, R.; Khalid-Naciri, J.; Idrissi, A. I. Effects Viscous Dissipation on the Asymptotic Behaviour of Laminar Forced Convection for HerscheI-Bulkley Fluid in a Circular Duct. *J. Mech. Eng. Autom.* **2016**, *6*, 419−426.
(35) Balhoff, M. T.; Thompson, K. E. Modeling the steady flow of yield stress flfluids in packed beds. *AIChE J.* **2004**, *50*, 3034−3048.
(36) Spiecker, P. M.; Gawrys, K. L.; Trail, C. B.; Kilpatrick, P. K. Effects of petroleum resins on asphaltene aggregation and water-in-oil emulsion formation. *Colloids Surf., A* **2003**, *220*, 9−27.
(37) Fingas, M.; Fieldhouse, B. Studies on crude oil and petroleum product emulsions: Water resolution and rheology. *Colloids Surf., A* **2009**, *333*, 67−81.
(38) Hou, Z. Z. *Study on Colloidal Chemical Properties of Ultra-Heavy Oil*; China University of Petroleum, 2010.
(39) Rodríguez de Castro, A.; Radilla, G. Flow of yield stress and Carreau fluids through rough-walled rock fractures: Prediction and experiments. *Water Resour. Res.* **2017**, *53*, 6197−6217.
(40) Bassane, J. F. P.; Sad, C. M. S.; Neto, D. M. C.; Santos, F. D.; Silva, M.; Tozzi, F. C.; Filgueiras, P. R.; de Castro, E. V. R.; Romão, W.; Santos, M. F. P.; da Silva, J. O. R.; Lacerda, V. Study of the Effect of Temperature and Gas Condensate Addition on the Viscosity of Heavy Oils. *J. Pet. Sci. Eng.* **2016**, *142*, 163−169.
(41) Zhang, D. Y.; Peng, J.; Gu, Y. L. Experiment of the threshold pressure gradient in heavy oil reservoir. *Xinjiang Shiyou Dizhi* **2012**, *2*, 201−204.
(42) Xu, J. F. *Study on Seepage Law of Ordinary Heavy Oil Considering the Threshold Pressure Gradient*; China University of Petroleum: Beijing, 2007.
(43) Wu, Z. H. *Study on Distribution Law of Remaining Oil in Heavy Oil Reservoir in Chenjiazhuang Oilfield*; China University of Petroleum: East China, 2016.
(44) Sun, J. F. Threshold pressure gradient study on non-Newtonian flow of heavy oil reservoirs in Shengli oilfield. *Youqi Dizhi Yu Caishoulu* **2010**, *17*, 74−77.
(45) Shan, C. X.; Wang, D. C. Experimental study on the threshold pressure gradient. *Oil & Gas Field Surface Engineering* **2010**, *29*, 30−32.
(46) Tian, J.; Xu, J. F.; Cheng, L. S. The Method of Characterization and Physical Simulation of TPG for Ordinary Heavy Oil. *J. Southwest Pet. Univ.* **2009**, *31*, 158−162.
(47) Li, A. F.; Zhang, S. H.; Liu, M.; Wang, W. G.; Zhang, L. A New Method of Measuring threshold Pressure for Low Permeability Reservoir. *J. China Univ. Pet., Ed. Nat. Sci.* **2008**, *32*, 68−71.
(48) Ke, W. L.; Wang, W. Y.; You, Y. Research of nonlinear seepage threshold pressure gradient determine method. *Shiyou Huagong Yingyong* **2013**, *32*, 1−4.
(49) Ke, W. L.; Yu, G. M. Experimental study of nonlinear seepage for heavy oil. *Shiyou Shiyan Dizhi* **2013**, *4*, 464−467.
(50) Xin, X. K. *Study of Numerical Simulation with Water Flooding Heavy Oil Reservoir Based on Nonlinear Seepage*; Yangtze University, 2013.

https://doi.org/10.1021/acsomega.1c04537
ACS Omega 2022, 7, 3949−3962